Published in final edited form as:
Exp Eye Res. 2009 March ; 88(3): 418–425. doi:10.1016/j.exer.2008.10.010.

Transscleral iontophoretic and intravitreal delivery of a macromolecule: Study of ocular distribution *in vivo* and postmortem with MRI

Sarah A. Molokhia[a], **Eun-Kee Jeong**[b], **William I. Higuchi**[a], and **S. Kevin Li**[c,*]

[a]Department of Pharmaceutics and Pharmaceutical Chemistry, College of Pharmacy, University of Utah, UT 84112, USA

[b]Department of Radiology and Utah Center for Advanced Imaging Research, University of Utah, Salt Lake City, UT 84108, USA

[c]Division of Pharmaceutical Sciences, College of Pharmacy, University of Cincinnati, 3225 Eden Ave, HPB 136, Cincinnati, OH 45267, USA

Abstract

The distribution and clearance of macromolecules in ocular delivery are not well understood. It has been hypothesized that iontophoresis can enhance transscleral delivery of macromolecules. The objective of this study was to investigate the ocular distribution of a macromolecule after transscleral iontophoretic delivery and intravitreal injection *in vivo* using nuclear magnetic resonance imaging (MRI) and to compare these results. Experiments of constant current transscleral iontophoresis of 4 mA or intravitreal injection were performed on New Zealand white rabbits *in vivo*. Iontophoresis experiments were also performed on rabbits postmortem. Galbumin™ (Gd-labeled albumin) was the model permeant surrogate to clinical therapeutic agents. MRI was used to monitor the distribution of the molecule in the eye after ocular iontophoresis and intravitreal injection. In addition, the conjunctiva, sclera, choroid, and retina were extracted in the transscleral iontophoresis study to determine the amounts of Galbumin™ in these tissues using Inductively Coupled Plasma Optical Emission Spectroscopy (ICP-OES). The results show that iontophoresis enhanced the ocular delivery of Galbumin™. The macromolecule was mainly delivered into the conjunctiva and sclera in microgram quantities and then diffused towards the posterior section in the upper hemisphere of the eye *in vivo*. Both *in vivo* and postmortem studies show that the iontophoretic delivery of Galbumin™ into the vitreous was below the detection limit. In the intravitreal injection study, the diffusion coefficient of Galbumin™ in the vitreous humor was estimated to be close to that of free aqueous diffusion.

Keywords

ocular; drug delivery; MRI; iontophoresis; intravitreal injection; pharmacokinetics

1. Introduction

Previous MRI studies using manganese ion (Mn^{2+}) and Mn^{2+} with ethylenediaminetetraacetic acid (EDTA) chelate have revealed the ocular barriers to transscleral drug delivery and

*Corresponding author. Tel.: +1 513 558 0977; fax: +1 513 558 0978. *E-mail address:* kevin.li@uc.edu (S.K. Li).

contributed to the understanding of the mechanisms of ocular iontophoresis (Li et al., 2004a,b; Molokhia et al., 2007, 2008). There were several advantages of using Mn^{2+} and EDTA chelate. First, the high paramagnetism of Mn^{2+} provided good MRI signal enhancement and allowed the use of practically low concentration of $MnCl_2$ solution. Second, the transport pathways of Mn^{2+} and $MnEDTA^{2-}$ penetrating the eye during iontophoresis could be used to study the electric current pathways in ocular iontophoresis. Third, free Mn^{2+} (contrary to free gadolinium ion) showed no significant binding to proteins in the vitreous. However, Mn^{2+} and $MnEDTA^{2-}$ are small ions that can easily penetrate ocular barriers that larger molecules cannot. It is unclear if the Mn^{2+} and $MnEDTA^{2-}$ data can be extrapolated to macromolecules and therapeutic agents in ocular drug delivery, particularly in ocular iontophoresis.

For macromolecule delivery, it is generally believed that the diffusion and electromigration of macromolecules depend mainly on their molecular sizes and charges. The pharmacokinetics of macromolecules in the eye is likely to be related to these factors unless facilitated/active transport such as endocytosis is involved. Surrogate permeants of therapeutic agents allow scientists to envision what can ultimately be delivered by ocular iontophoresis in clinical studies. It has been shown that the internal membrane of the retina impedes diffusion of linear molecules larger than 40 kDa and globular molecules larger than 70 kDa (Smelser et al., 1965; Peyman and Bok, 1972; Marmor et al., 1985; Kamei et al., 1999), precluding intravitreous delivery of many antiangiogenic macromolecular drugs under development. However, intravitreal injection of bevacizumab (Avastin®) which has molecular weight 3 times that of ranibizumab (Lucentis®) had resulted in a significant decrease in macular edema and improvement in visual acuity (Lang, 1995; Iturralde et al., 2006). The macromolecule selected in the present study Galbumin™ has a molecular weight approximately 1.5 times that of Macugen® (≈ 50 kDa) and Lucentis® (≈48 kDa). This compound could serve as a surrogate adequate for the study and the understanding of the migration and distribution of these macromolecules in the eye during transscleral iontophoresis and intravitreal injection.

Recent interest in drug delivery to the back of the eye has stimulated new interest in ocular iontophoresis. In ocular iontophoresis, a donor electrode containing the drug to be delivered into the eye is placed on the eye. To complete an electrical circuit, another electrode is placed on another body surface. Ocular iontophoresis does not have some of the adverse effects associated with intravitreal and periocular injections such as retinal detachment, endophthalmitis, globe perforation and ptosis (Haupert and Jaffe, 2000; Antcliff et al., 2001). Ocular iontophoresis has also been shown to enhance the delivery of a broad range of drugs into the eye such as antibiotics (Vollmer et al., 2002; Eljarrat-Binstock et al., 2004), corticosteroids (Lam et al., 1989; Eljarrat-Binstock et al., 2008), non-steroidal antiinflammatory agents (Voigt et al., 2002; Kralinger et al., 2003), and immunosuppressants (Eljarrat-Binstock et al., 2007). The existing devices were also shown to be effective in the treatment of certain eye diseases and without known side effects (Voigt et al., 2002; Yoo et al., 2002; Parkinson et al., 2003). Most transscleral iontophoresis studies have been focused on the delivery of small molecules with only a few studies on macromolecules. Particularly, the barriers, distribution, and penetration of macromolecules into the eye are not well understood.

The objectives of the present study were to examine the delivery of a model macromolecule into the eye in transscleral iontophoresis and to determine the distribution of this macromolecule after intravitreal injection *in vivo*. Postmortem experiments were also conducted to assess the transscleral barrier without the interference of ocular clearance. The outcome of this study was expected to provide insights into the distribution and clearance of macromolecular therapeutic agents for future ocular drug delivery development.

2. Experimental section

2.1. Materials

Galbumin™ (25 mg/ml) was purchased from BioPAL, Inc. (Worcester, MA). Galbumin™ is a bovine albumin conjugated with gadolinium (Gd). It has approximately 10–15 Gd atoms per albumin unit. It is a globular protein with an estimated net negative charge of 27. Spectra/Gel® absorbent (polyacrylate-polyalcohol) and dialysis tubing were both purchased from Spectrum® Labs, Inc. (Rancho Dominguez, CA). Gadolinium atomic absorption standard solution (1005 ppm of Gd in 1.0 wt% HNO_3) was purchased from Aldrich (St. Louis, MO).

2.2. Galbumin™ characterization and preparation

Matrix-assisted laser desorption/ionization time of flight mass spectroscopy (MALDI-TOF) was used to determine the molecular weight distribution of Galbumin™. For the purpose of the present study, the free aqueous diffusion coefficient (D) of Galbumin™ was determined under the assumption that Galbumin™ has similar frictional coefficient ratio as bovine serum albumin (BSA). The diffusion coefficient of BSA at 20°C in pure water is 6.1×10^{-7} cm^2/s (Cantor and Schimmel, 1980). The free aqueous diffusion coefficient of Galbumin™ at 37°C ($D_{Galbumin}$) was calculated using the diffusion coefficient of BSA (D_{BSA}) and correcting for the molecular weight difference and the viscosity of water at 37°C.

$$D_{\text{Galbumin}} = D_{\text{BSA}} \frac{\eta_{20^\circ\text{C}}}{\eta_{37^\circ\text{C}}} \left(\frac{M_{\text{BSA}}}{M_{\text{Galbumin}}} \right)^{1/3} \quad (1)$$

where $\eta_{20°C}$ is the viscosity of water at 20 °C, $\eta_{37°C}$ is the viscosity of water at 37 °C, M_{BSA} is the molecular weight of BSA, and $M_{Galbumin}$ is the molecular weight of Galbumin™.

To concentrate the Galbumin™ solution, Galbumin™ was pipetted into a Spectra/Por® dialysis tubing of 1000 Da molecular weight cut off and covered with spectra/gel absorbent. Galbumin™ was concentrated to approximately 100 mg/ml for the transscleral iontophoresis experiments.

2.3. Iontophoresis device

The iontophoresis device was obtained from Aciont, Inc. (Salt Lake City, UT). The electrode device was made of silicone polymer and has a lens shaped design for application onto a rabbit eye (Miller et al., 2008). The device had three drug delivery chambers (about 2 mm apart). This lens shaped design permitted direct contact of these chambers with the bulbar conjunctiva adjacent to the limbus. In the present study, only the middle chamber which contained a Ag/AgCl electrode was used for Galbumin™ delivery. Instrument Wipe, 2 mm thickness, was purchased from Ivalon® and circular discs (diameter approximately 0.07 cm^2) were cut out from the wipe and left to equilibrate in the Galbumin™ solution for at least 24 h.

2.4. *In vivo* transscleral iontophoresis and intravitreal injections

New Zealand white rabbits of 3–4 kg were purchased from Western Oregon Rabbit Co. (Philomath, OR) and were used in the experiments under the approval of the Institutional Animal Care and Use Committee at the University of Utah. After the rabbits were anesthetized with 25–50 mg/kg ketamine IM and 5–10 mg/kg xylazine IM, the lens device was placed on the conjunctiva/sclera in the superior cul-de-sac (under the upper eyelid) near the limbus at the pars plana. The return electrode (approximately 4 cm^2 surface area) was placed on a section of gauze pad (approximately 40 cm^2 surface area) wetted in saline and clamped to the ear on the side opposite to that of the treated eye. The Galbumin™ solution soaked Ivalon® wipe was

placed in the middle chamber of the device. When the device was applied on the eye, this wipe was in direct contact with the bulbar conjunctiva. Cathodal iontophoresis was performed on the eye using constant direct current of 4 mA for 20 min. Rabbits without any treatments were the control. Passive delivery using the Galbumin™-loaded device without the application of an electric field was another control.

Intravitreal injections of Galbumin™ were carried out at concentrations of 0.25,1, and 4 mg/ml using a 29-gauge needle. The volume used in the injection was 0.1 ml. The injection site was the pars plana approximately 3 mm away from the limbus. In the analysis of the intravitreal injection data, a simple model of passive diffusion from a spherical source (Li et al., 2004a) was used to study the early distribution of Galbumin™ from the injection site in the vitreous. Briefly, this analysis assumed that the bolus injection initially created a 0.1 ml sphere of equally distributed Galbumin™ in the vitreous, and that the concentration at radial position r at time t (C_r) from the center of an initially uniformly distributed spherical source of concentration C_0 and radius a was related to the diffusion coefficient according to:

$$C_r = \frac{1}{2}C_0\left(\operatorname{erf}\frac{a-r}{2\sqrt{Dt}} + \operatorname{erf}\frac{a+r}{2\sqrt{Dt}}\right) - \frac{C_0}{r}\sqrt{\frac{Dt}{\pi}}\left\{\exp\left(\frac{-(a-r)^2}{4Dt}\right) - \exp\left(\frac{-(a+r)^2}{4Dt}\right)\right\} \quad (2)$$

The *in vivo* diffusion coefficient of Galbumin™ could then be determined using these parameters and equation (2).

2.5. Postmortem iontophoresis studies

The purpose of the postmortem studies was to assess the transscleral barrier without ocular clearance (e.g., vasculature and lymphatic clearance). Previous studies have suggested that ocular clearance is a major barrier in transscleral transport and experiments with animals postmortem would allow the identification of the importance of this barrier (Kim et al., 2004; Li et al., 2004b; Molokhia et al., 2008). In the present study, experiments of Gal-bumin™ in postmortem rabbits were conducted approximately 5–10 min after sacrificing the rabbits. The procedure of transscleral iontophoresis on the postmortem rabbits was the same as that described in the *in vivo* study. After iontophoresis, the animals were left at room temperature for up to 24 h.

2.6. MRI calibration

Experiments were conducted to generate a calibration curve of Galbumin™ enhanced signal intensity versus Galbumin™ concentration as described previously (Li et al., 2004a,b). Briefly, Galbumin™ standard solutions of 0.025–12.5 mg/ml were prepared in saline. The solutions (~ 1 ml) in HPLC vials were imaged with spinecho pulse sequences: TR was 50, 100, 200, 400, 800, 1600, 2400, and 3200 ms with TE fixed at 13 ms for T_1 measurement, and TE was 9, 18, 27, 36, 45, 54, 63, 72, and 82 ms with TR fixed at 3000 ms for T_2 measurement. The relaxation times T_1 and T_2 of these standards were determined by curve fitting of the signal intensity of a region of interest (ROI) with respect to the time variables TR and TE using the signal equation of the spin-echo imaging (Li et al., 2004b):

$$\frac{S_I}{S_o} = \left(1 - e^{-TR/T_1}\right)e^{-TE/T_2} \quad (3)$$

where S_I is the signal intensity, S_o is the intrinsic fully recovered signal intensity, T_1 is the spin-lattice relaxation time, and T_2 is the spin-spin relaxation time.

2.7. Animal MRI

In the *in vivo* study, the animals were anesthetized (re-anesthetized) as described in "*in vivo* transscleral iontophoresis and intravitreal injections" before each MRI scan. In the postmortem study, the animals were scanned directly at the predetermined time points. MRI experiment was conducted in a clinical 3-T MRI system (Trio with Avanto gradient, Siemens Medical Solution, Erlangen, Germany) with a human wrist coil (a transmit/receive volume coil). MR imaging was performed with T_1 weighted spin-echo imaging technique. The imaging parameters were 675 ms TR, 13 ms TE, 12 signal averages, FOV of 90 mm and fat suppression. The slice thickness was 1.0 mm with no spacing. The spatial resolution was 0.28 × 0.28 × 1.0 mm^3. Each scan provided at least twenty transaxial image slices to cover the whole eye. Imaging time for single time data was approximately 26 min. The MR images were analyzed with MRIcro and Image J (obtained from MRIcro and NIH websites).

2.8. Traditional ocular pharmacokinetics

A traditional ocular pharmacokinetic study was performed to verify the MRI data. The rabbits were sacrificed at either 30 min or 12 h after transscleral iontophoresis. Both eyes were then enucleated. The eye was dissected using a surgical scalpel. The conjunctiva and sclera composite tissues were removed separately from the upper hemisphere region underneath the electrode. The conjunctiva composite (C/M composite) included the conjunctiva and superior muscle. The sclera composite (S/C/R composite) included the sclera, choroid and retina tissues. After eye excision, the eye tissues were left in 5 ml saline for 24 h at 4 °C. A second extraction of the same eye tissues was performed using 5 ml saline for another 24 h, which was followed by a third extraction using the same procedure. The extraction method was validated by spiking the tissues with a known amount of Galbumin™. The first two extractions retrieved 95% of the total amount while the third extraction retrieved less than 1% of the total.

The concentrations of Galbumin™ in the C/M and S/C/R composites were determined using Inductively Coupled Plasma Optical Emission Spectroscopy (ICP-OES) at wavelength 342.247 nm in Gd assay:

$$\frac{\text{Intensity(sample)} - \text{Intensity(saline)}}{\text{Intensity(std, 1 ppm)}} = \text{concentration (sample) ppm} \quad (4)$$

To confirm that the observed signal in MRI experiments was from the Gd linked to albumin (from Galbumin™) and not free Gd ions, the extracted solution (from eye tissues) was centrifuged in an Amicon centrifugal tube with molecular weight cut off 10 kDa. Samples from the filtrate were checked for Gd content. The filtrate showed negligible amount of Gd present implying the absence of free Gd^{3+} ions in the extracted solution. A positive control (i.e., standard Galbumin™) was checked for free Gd^{3+} and negligible amount of Gd was found in the filtrate. Also, a standard Gd atomic absorption solution (free Gd^{3+} ions) diluted to 2 ppm in water was filtered with the 10 kDa molecular weight cut off centrifugal tube and showed 91% ± 2% recovery in the filtrate.

3. Results

3.1. Galbumin™ characterization

The MALDI-TOF spectrum of Galbumin™ showed average molecular weight of 80 kDa. Other peaks at 40, 24, and 20 kDa represented the double, triple, and quaternary charge ion dissociation, respectively. The free aqueous diffusion coefficient of Galbumin™ in water at

37°C was estimated to be 8×10^{-7} cm^2/s using the diffusion coefficient of BSA, viscosity of water at 20° and 37°C, and Galbumin™ and BSA molecular weights (see equation (1)).

3.2. MRI calibration

Fig. 1a and b shows the relationships of the relaxation rates $1/T_1$ and $1/T_2$ versus Galbumin™ concentration in saline. Linear relationships between the relaxation rates and Galbumin™ concentration were observed. The *y*-intercept of the $1/T_1$ versus concentration plot is consistent with T_1 of saline/water in the literature (~3–4 s).

Fig. 2 shows the ratio of S_I/S_o versus Galbumin™ concentrations in saline. The S_I/S_o ratio was calculated using the experimental T_1 and T_2 measured at each concentration, 675 ms TR, 13 ms TE, and equation (3). The S_I/S_o reached a maximum of approximately 0.86 at around 4 mg/ml Galbumin™ and was relatively linear at lower concentration. The concentration of Galbumin™ used for intravitreal injection was therefore chosen to be 0.25 and 1 mg/ml. 4 mg/ml Galbumin™ was also used but the data were not included in the pharmacokinetic analysis. Fig. 2 also shows the S_I/S_o value divided by the S_I/S_o background versus Galbumin™ concentration. The S_I/S_o background value was approximately 0.2 in the MR images.

3.3. *In vivo* MRI

Iontophoresis significantly enhanced the delivery of Galbumin™ as there was no ocular tissue penetration observed in the passive delivery control experiment (without the application of iontophoresis, Fig. 3). Fig. 3 also presents the MR images in the 20-min 4-mA transscleral iontophoresis study. As observed in the images, Galbumin™ was mainly delivered to the conjunctiva and nearby tissues. No Galbumin™ was detected in the anterior chamber or vitreous over the duration of the study. The site of delivery was mainly located below the electrode.

Fig. 4 shows the MR images in the 0.25,1, and 4 mg/ml Galbumin™ intravitreal injection study. The injection spot was in the vitreous usually towards the back of the eye near the retina. When the injection spot was closer to the lens, the spreading of Galbumin™ behind the lens was suggestive of a less resistive region to the flow of the solution introduced by the needle into this region during injection (Fig. 4b). Within 4 h after injection, Galbumin™ rapidly diffused from the spot of the injection and spread in the vitreous. At 24 h, the macromolecule almost completely filled the vitreous humor. No significant amount of Galbumin™ was detected in the anterior chamber over the duration of the study.

To quantitatively study the diffusion of Galbumin™ in the eye after intravitreal injection, the signal intensity in the ROI, which was the position of injection and had the highest concentration of Galbumin™ (highest signal), was monitored. Fig. 5 shows that the signal at the ROI dropped rapidly in the first 4 h followed by a slower decrease from 10 to 60 h. The diffusivity of Galbumin™ in the vitreous after intravitreal injections was estimated using equation (2) to be 8×10^{-7} cm^2/s (uncertainty: $\pm 3 \times 10^{-7}$ cm^2/s), essentially the same as its free aqueous diffusion coefficient (8×10^{-7} cm^2/s; see Section 3.1).

To study the clearance of Galbumin™ in the vitreous, Fig. 6 presents the total signal in the vitreous at approximately 0.4, 4, 12, 23, 40, and 60 h after injection with the assumption that the signal intensity is proportional to Galbumin™ concentration. This is a reasonable assumption at the low Galbumin™ concentrations (≤1 mg/ml) used in the present study (see Fig. 2). As a result, the 4 mg/ml data were not included in the present analysis. Within the data scatter, the clearance of Galbumin™ in the vitreous (up to 60 h) after the 0.25 and 1 mg/ml injections can be interpreted as zeroth-order clearance ($r^2 \geq 0.57$). A comparison of the 0.25 and 1 mg/ml data further supports that the clearance follows zeroth-order kinetics - the rates

of the decrease in the total vitreous concentration of Galbumin™ after 0.25 and 1 mg/ml injections are not significantly different (average rate = −15 and −18 total MRI signal/h, respectively). In summary, the present results are consistent with slow Galbumin™ clearance in the vitreous with a half-life of approximately 2 days after 1 mg/ml injection and 0.7 day after 0.25 mg/ml injection with a substantial amount of Galbumin™ still present in the vitreous over the duration of the study.

3.4. Postmortem MRI

In transscleral iontophoresis postmortem, deeper penetration reaching approximately 3 mm underneath the electrode (e.g., deeper into the ciliary body) than that *in vivo* was observed in the earlier time ~1 h after iontophoresis (Fig. 7). The clearance of Galbumin™ in the postmortem study was also found to be slower than that *in vivo*. Similar to the results in the *in vivo* study, no penetration of the macromolecule into the vitreous was detected postmortem. It was also noted that some eyes were slightly deformed at > 13 h after the animals were sacrificed, indicated by the unusual eye shapes seen in a few MR images at these later time points. Although the eye tissues were suggested to remain viable several hours postmortem (Kim et al., 2004), caution must be exercised in the interpretation of the postmortem results, especially at the later time points, due to potential postmortem tissue changes and the lower body temperature postmortem than *in vivo*.

3.5. *In vivo* traditional pharmacokinetics

Table 1 shows the amount of Galbumin™ in the C/M and S/C/R tissue composites within approximately 0.4 cm^2 around the site of electrode application at 30 min and 12 h after 20-min 4-mA transscleral iontophoresis *in vivo*. These results are consistent with the MRI results and show that most of the Galbumin™ delivery occurs in the conjunctiva region. Smaller amounts of Galbumin™ were found to be present in the S/C/R composite. The pharmacokinetic data show that the amount of Galbumin™ in the C/M and S/C/R composites at 30 min after transscleral iontophoresis ($n \geq 3$) was in the range of 19–38 and 9–17 μg, respectively. At 12 h after iontophoresis, the remaining amount of Galbumin™ in the C/M composite was approximately 2.9–4.5 μg and that in the S/C/R composite was 0.3–5.2 μg. Assuming that the concentration of Galbumin™ in the sponge was 100 mg/ml, with 20 μl volume, the total amount of Galbumin™ in the iontophoresis device was 2 mg. The amounts delivered to the C/M and S/C/R composites at 30 min after iontophoresis therefore correspond to approximately 1–2% and 0.4–1% of the total dose in the device, respectively.

4. Discussion

4.1. Ocular delivery and distribution after iontophoresis

In the present study, transscleral iontophoretic delivery of Galbumin™ to the conjunctiva and sclera was demonstrated. The delivery of the macromolecule was primarily to the conjunctiva and nearby tissue below the site of iontophoresis application. No Galbumin™ was detected in the vitreous (i.e., below the detection limit) in both the *in vivo* and postmortem studies. A possible explanation is that the retinal pigmented epithelium barrier does not allow any significant penetration of the macromolecule (80 kDa globular protein) used in the present study. Clearance such as blood vasculature and lymphatic clearance may also reduce iontophoretic macromolecular delivery (Kim et al., 2004; Robinson et al., 2006; Molokhia et al., 2008). Previous studies have proposed that small molecules are mainly eliminated by the blood capillaries and macromolecules such as Galbumin™ (radius ≈ 4 nm) are cleared primarily by the lymphatic system (Supersaxo et al., 1990; McLennan et al., 2005; Kim et al., 2008). In the present study, the pharmacokinetic data at 12 h after iontophoresis show that the clearance of Galbumin™ in the C/M tissues is faster than that in the S/C/R tissues (Table 1). A comparison of the present and previous pharmacokinetic data suggests that the difference

between the half-lives of the small molecules in the previous studies and Galbumin™ in the present study is related to their diffusion coefficients. For example, an approximately 10× decrease in the concentration of small molecules in the conjunctiva and sclera was observed in the first 2 h after delivery (Kondo and Araie, 1989; Voigt et al., 2002), suggesting initial elimination half-lives of around 0.6 h in these tissues. The half-life of Galbumin™ clearance in the same tissues was approximately 5 h in the present study, which is roughly 8× longer than those of the small molecules (free aqueous diffusion coefficients of these small molecules and Galbumin™ were ~6×10^{-6} cm^2/s and 8×10^{-7} cm^2/s, respectively). This suggests that tissue clearance was mainly diffusion-controlled. The present postmortem data also suggest that the dynamic barrier (i.e., clearance) is not the main factor for the lack of Galbumin™ penetration into the vitreous. This is consistent with the previous observation that the rate of clearance after subconjunctival injection of Gd-DTPA *in vivo* was substantially higher than that postmortem, but the *in vivo* and postmortem clearance rates of Galbumin™ did not differ significantly (Kim et al., 2008). Similarly for iontophoretic delivery, although significant enhancement of small molecule delivery into the vitreous was previously observed postmortem (compared to those *in vivo*) after iontophoresis (Molokhia et al., 2008), there was no significant enhancement in Galbumin™ delivery into the vitreous postmortem versus *in vivo* in the present study.

Although Galbumin™ was not observed in the vitreous in the present study, the delivery of macromolecules from the conjunctiva and sclera to the posterior retina cannot be ruled out. Literature has shown that drugs delivered by intrascleral injection or implant could reach the retina and choroid via the suprachoroidal space (Gilger et al., 2006; Kim et al., 2007). This suggests that the delivery of a drug into and across the sclera could eventually result in the delivery of the drug to the choroid and retina. The results in the present study suggest the possibility of using transscleral iontophoresis to deliver macromolecules into these posterior tissues. Future studies are needed to test this hypothesis and to optimize the electrode position, the current intensity, and the duration of iontophoresis for transscleral iontophoretic delivery of macromolecules.

4.2. Ocular distribution after intravitreal injection

The diffusion of Galbumin™ in the rabbit vitreous was fast after intravitreal injection. Within 24 h after the injection, the macromolecule was observed to fill almost the whole vitreous independent of the variability associated with the injection location. Despite the relatively high viscosity of the vitreous humor (Xu et al., 2000), no significant hindrance of Galbumin™ diffusion was observed in the vitreous; the diffusion coefficient of Galbumin™ in the vitreous based on equation (2) was essentially the same as that in free aqueous diffusion. This is consistent with previous studies of small permeants (Berkowitz et al., 1994; Xu et al., 2000; Li et al., 2004a) and radioactive proteins (Maurice, 1959). Together, the previous and present findings suggest that the microscopic viscosity of vitreous humor is similar to that of saline/water and that the hyaluronic acid in rabbit eyes, providing the viscosity of the vitreous humor, may not create a polymer network dense enough to significantly hinder Galbumin™ diffusion. The present results show that the half-life of the macro-molecule (free aqueous diffusion coefficient ≈ 8×10^{-7} cm^2/s) is concentration dependent and approximately 2 days after the 1 mg/ml injection.

It has been suggested that drugs are eliminated by two main routes after intravitreal injection: anterior and posterior (Worakul and Robinson, 1997; Maurice, 2001; Urtti, 2006). In general, hydrophilic drugs have been suggested to utilize the anterior route and lipophilic drugs the posterior route (Worakul and Robinson, 1997). In the anterior route, the drug diffuses across the vitreous to the posterior chamber and, thereafter, cleared from the posterior and anterior chambers. Elimination can then be through uveal blood flow or Schlemm's canal in the anterior chamber although a previous study did not find Gd-albumin permeation across the blood-

aqueous barrier (Wu et al., 1992). In the posterior route, the drug is eliminated across the blood-retina barrier into the blood circulation. Therefore, posterior elimination requires the permeation of the drug across the retinal pigmented epithelium in the blood-retina barrier, and molecules with high molecular weight and high water-solubility tend to have long half-lives in the vitreous (Urtti, 2006). The present data show no significant increase in Galbumin™ concentration in the anterior chamber in the MR images after 0.25 and 1 mg/ml injections. In the 4 mg/ml intravitreal injection study, a slight increase in anterior chamber signal was observed (Fig. 4) but the increase was not statistically significant. The present results suggest that (a) the concentration of the macromolecule in the anterior chamber was below detection due to the fast aqueous humor turnover and slow diffusion from the vitreous to the anterior chamber, (b) clearance occurred at the uvea/ciliary body as the main elimination pathway before the accumulation of the macromolecule in the anterior chamber, or (c) posterior clearance remained the main ocular elimination route for the macromolecule.

4.3. Ocular drug delivery in human

Although the rabbit is the most commonly used animal model for ocular research due to its similarities to human such as permeability characteristics and anterior chamber volume, there are major differences between the rabbit and human eye tissues (Mitra, 2003). For example, the thickness of the sclera in the New Zealand rabbits is between 0.2 and 0.3 mm at equator whereas that in humans is 0.4–0.5 mm. The volume of the vitreous humor in rabbits is approximately 1.5 ml, smaller than the volume of 4 ml in humans. The components of vitreous humor such as hyaluronic acid can also be different in animals and humans, and the vitreous humor properties such as viscosity can change with age and disease states. As a result, there are limitations in extrapolating the results in the present study to human. For example, in the intravitreal injection study, if vitreous clearance is diffusion-controlled or via the anterior route, the rate of clearance can be slower in humans due to the larger volume of human vitreous compared to the rabbit. On the contrary, if the clearance is barrier-controlled via the posterior route, the rate of clearance can be faster in humans due to the larger retinal surface area when the permeability of the retina-blood barrier is the same. Despite this, some data obtained in rabbits can be useful to understand the mechanisms of ocular drug delivery such as the location and distribution of Galbumin™ in the eye after iontophoresis application and the pathway of Galbumin™ clearance after intravitreal injection. At the anatomical and histological levels, human and rabbit vitreous matrices are sufficiently similar to make the rabbit a promising animal model for the study of vitreous matrix differentiation and degeneration (Los, 2008). In summary, caution should be exercised to utilize the present results in ocular delivery development.

5. Conclusion

The distribution of a globular macromolecule in the eye was studied with MRI after transscleral iontophoresis and intravitreal injection. Traditional pharmacokinetic study was also conducted. The results in the present study with Galbumin™ provide insights into the distribution and clearance of macromolecules of sizes and shapes similar to those of ranibizumab in ocular drug delivery. In the iontophoresis study, the potential of using iontophoresis as a noninvasive delivery method for macromolecules to the posterior segment of the eye was investigated. Transscleral iontophoresis primarily delivered the macromolecule to the conjunctiva and nearby tissues under the site of the iontophoresis application. No Galbumin™ was detected in the anterior chamber or vitreous after iontophoresis. At 12 h after iontophoresis, a significant amount of Galbumin™ was cleared from the tissues. In the intravitreal injection study, the distribution of Galbumin™ in the vitreous humor was fast with a diffusion coefficient estimated to be close to that of free aqueous diffusion.

Acknowledgements

This research was supported by NIH Grant EY 015181. The authors thank Xin Liu for his help in the MRI experiments and Aciont Inc. (Salt Lake City, UT) for providing the iontophoresis electrode device. The authors also thank Dr. Steven Kern, Dr. James Herron, and Dr. Paul Bernstein for their helpful discussions and Dr. Paul Cobine for his help with the ICP-OES.

References

Antcliff RJ, Spalton DJ, Stanford MR, Graham EM, ffytche TJ, Marshall J. Intravitreal triamcinolone for uveitic cystoid macular edema: an optical coherence tomography study. Ophthalmology 2001;108:765–772. [PubMed: 11297495]

Berkowitz BA, Wilson CA, Tofts PS, Peshock RM. Effect of vitreous fluidity on the measurement of blood-retinal barrier permeability using contrast-enhanced MRI. Magn. Reson. Med 1994;31:61–66. [PubMed: 8121271]

Cantor, CR.; Schimmel, PR. Biophysical Chemistry: Part II: Techniques for the Study of Biological Structure and Function. Vol. first ed. W.H. Freeman; 1980.

Eljarrat-Binstock E, Domb AJ, Orucov F, Frucht-Pery J, Pe'er J. Methotrexate delivery to the eye using transscleral hydrogel iontophoresis. Curr. Eye Res 2007;32:639–646. [PubMed: 17852187]

Eljarrat-Binstock E, Orucov F, Frucht-Pery J, Pe'er J, Domb AJ. Methyl-prednisolone delivery to the back of the eye using hydrogel iontophoresis. J. Ocul. Pharmacol. Ther 2008;24:344–350. [PubMed: 18476804]

Eljarrat-Binstock E, Raiskup F, Stepensky D, Domb AJ, Frucht-Pery J. Delivery of gentamicin to the rabbit eye by drug-loaded hydrogel iontophoresis. Invest. Ophthalmol. Vis. Sci 2004;45:2543–2548. [PubMed: 15277475]

Gilger BC, Salmon JH, Wilkie DA, Cruysberg LP, Kim J, Hayat M, Kim H, Kim S, Yuan P, Lee SS, Harrington SM, Murray PR, Edelhauser HF, Csaky KG, Robinson MR. A novel bioerodible deep scleral lamellar cyclosporine implant for uveitis. Invest. Ophthalmol. Vis. Sci 2006;47:2596–2605. [PubMed: 16723476]

Haupert CL, Jaffe GJ. New and emerging treatments for patients with uveitis. Int. Ophthalmol. Clin 2000;40:205–220. [PubMed: 10791266]

Iturralde D, Spaide RF, Meyerle CB, Klancnik JM, Yannuzzi LA, Fisher YL, Sorenson J, Slakter JS, Freund KB, Cooney M, Fine HF. Intravitreal bevacizumab (Avastin) treatment of macular edema in central retinal vein occlusion: a short-term study. Retina 2006;26:279–284. [PubMed: 16508427]

Kamei M, Misono K, Lewis H. A study of the ability of tissue plasminogen activator to diffuse into the subretinal space after intravitreal injection in rabbits. Am. J. Ophthalmol 1999;128:739–746. [PubMed: 10612511]

Kim H, Robinson MR, Lizak MJ, Tansey G, Lutz RJ, Yuan P, Wang NS, Csaky KG. Controlled drug release from an ocular implant: an evaluation using dynamic three-dimensional magnetic resonance imaging. Invest. Ophthalmol. Vis. Sci 2004;45:2722–2731. [PubMed: 15277497]

Kim SH, Csaky KG, Wang NS, Lutz RJ. Drug elimination kinetics following subconjunctival injection using dynamic contrast-enhanced magnetic resonance imaging. Pharm. Res 2008;25:512–520. [PubMed: 17674155]

Kim SH, Galban CJ, Lutz RJ, Dedrick RL, Csaky KG, Lizak MJ, Wang NS, Tansey G, Robinson MR. Assessment of subconjunctival and intrascleral drug delivery to the posterior segment using dynamic contrast-enhanced magnetic resonance imaging. Invest. Ophthalmol. Vis. Sci 2007;48:808–814. [PubMed: 17251481]

Kondo M, Araie M. Iontophoresis of 5-fluorouracil into the conjunctiva and sclera. Invest. Ophthalmol. Vis. Sci 1989;30:583–585. [PubMed: 2925327]

Kralinger MT, Voigt M, Kieselbach GF, Hamasaki D, Hayden BC, Parel JM. Ocular delivery of acetylsalicylic acid by repetitive coulomb-controlled iontophoresis. Ophthalmic Res 2003;35:102–110. [PubMed: 12646751]

Lam TT, Edward DP, Zhu XA, Tso MO. Transscleral iontophoresis of dexamethasone. Arch. Ophthalmol 1989;107:1368–1371. [PubMed: 2783069]

Lang JC. Ocular drug delivery conventional ocular formulations. Adv. Drug Deliv. Rev 1995;16:39–43.

Li SK, Jeong EK, Hastings MS. Magnetic resonance imaging study of current and ion delivery into the eye during transscleral and transcorneal iontophoresis. Invest. Ophthalmol. Vis. Sci 2004a;45:1224–1231. [PubMed: 15037591]

Li SK, Molokhia SA, Jeong EK. Assessment of subconjunctival delivery with model ionic permeants and magnetic resonance imaging. Pharm. Res 2004b;21:2175–2184. [PubMed: 15648248]

Los LI. The rabbit as an animal model for post-natal vitreous matrix differentiation and degeneration. Eye 2008;22:1223–1232. [PubMed: 18327158]

Marmor MF, Negi A, Maurice DM. Kinetics of macromolecules injected into the subretinal space. Exp. Eye Res 1985;40:687–696. [PubMed: 2408910]

Maurice DM. Protein dynamics in the eye studied with labelled proteins. Am. J. Ophthalmol 1959;47:361–368. [PubMed: 13617364]

Maurice DM. Review: practical issues in intravitreal drug delivery. J. Ocul. Pharmacol. Ther 2001;17:393–401. [PubMed: 11572470]

McLennan DN, Porter CJH, Charman SA. Subcutaneous drug delivery and the role of the lymphatics. Drug Discov. Today: Technol 2005;2:89–96.

Miller DJ, Li SK, Tuitupou AL, Kochambilli RP, Papangkorn K, Mix DCJ, Higuchi WI, Higuchi JW. Passive and oxymetazoline-enhanced delivery with a lens device: pharmacokinetics and efficacy studies with rabbits. J. Ocul. Pharmacol. Ther 2008;24:385–391. [PubMed: 18665810]

Mitra, AK. Ophthalmic Drug Delivery Systems. Vol. second ed. New York: Marcel Dekker; 2003.

Molokhia SA, Jeong EK, Higuchi WI, Li SK. Examination of penetration routes and distribution of ionic permeants during and after transscleral iontophoresis with magnetic resonance imaging. Int. J. Pharm 2007;335:46–53. [PubMed: 17236728]

Molokhia SA, Jeong EK, Higuchi WI, Li SK. Examination of barriers and barrier alteration in transscleral iontophoresis. J. Pharm. Sci 2008;97:831–844. [PubMed: 17879296]

Parkinson TM, Ferguson E, Febbraro S, Bakhtyari A, King M, Mundasad M. Tolerance of ocular iontophoresis in healthy volunteers. J. Ocul. Pharmacol. Ther 2003;19:145–151. [PubMed: 12804059]

Peyman GA, Bok D. Peroxidase diffusion in the normal and laser-coagulated primate retina. Investig. Ophthalmol 1972;11:35–45. [PubMed: 4621358]

Robinson MR, Lee SS, Kim H, Kim S, Lutz RJ, Galban C, Bungay PM, Yuan P, Wang NS, Kim J, Csaky KG. A rabbit model for assessing the ocular barriers to the transscleral delivery of triamcinolone acetonide. Exp. Eye Res 2006;82:479–487. [PubMed: 16168412]

Smelser, GK.; Ishikawa, T.; Pei, YF. Structure of the Eye. Stuttgart: Schattauer-Verlag; 1965.

Supersaxo A, Hein WR, Steffen H. Effect of molecular weight on the lymphatic absorption of water-soluble compounds following subcutaneous administration. Pharm. Res 1990;7:167–169. [PubMed: 2137911]

Urtti A. Challenges and obstacles of ocular pharmacokinetics and drug delivery. Adv. Drug Deliv. Rev 2006;58:1131–1135. [PubMed: 17097758]

Voigt M, Kralinger M, Kieselbach G, Chapon P, Anagnoste S, Hayden B, Parel JM. Ocular aspirin distribution: a comparison of intravenous, topical, and coulomb-controlled iontophoresis administration. Invest. Ophthalmol. Vis. Sci 2002;43:3299–3306. [PubMed: 12356838]

Vollmer DL, Szlek MA, Kolb K, Lloyd LB, Parkinson TM. In vivo transscleral iontophoresis of amikacin to rabbit eyes. J. Ocul. Pharmacol. Ther 2002;18:549–558. [PubMed: 12537681]

Worakul N, Robinson JR. Ocular pharmacokinetics/pharmacodynamics. Eur. J. Pharm. Biopharm 1997;44:71–83.

Wu JC, Jesmanowicz A, Hyde JS. Anterior segment high resolution MRI: aqueous humor dynamics observed using contrast agents. Exp. Eye Res 1992;54:145–148. [PubMed: 1541333]

Xu J, Heys JJ, Barocas VH, Randolph TW. Permeability and diffusion in vitreous humor: implications for drug delivery. Pharm. Res 2000;17:664–669. [PubMed: 10955838]

Yoo SH, Dursun D, Dubovy S, Miller D, Alfonso E, Forster RK, Behar-Cohen F, Parel JM. Iontophoresis for the treatment of paecilomyces keratitis. Cornea 2002;21:131–132. [PubMed: 11805526]

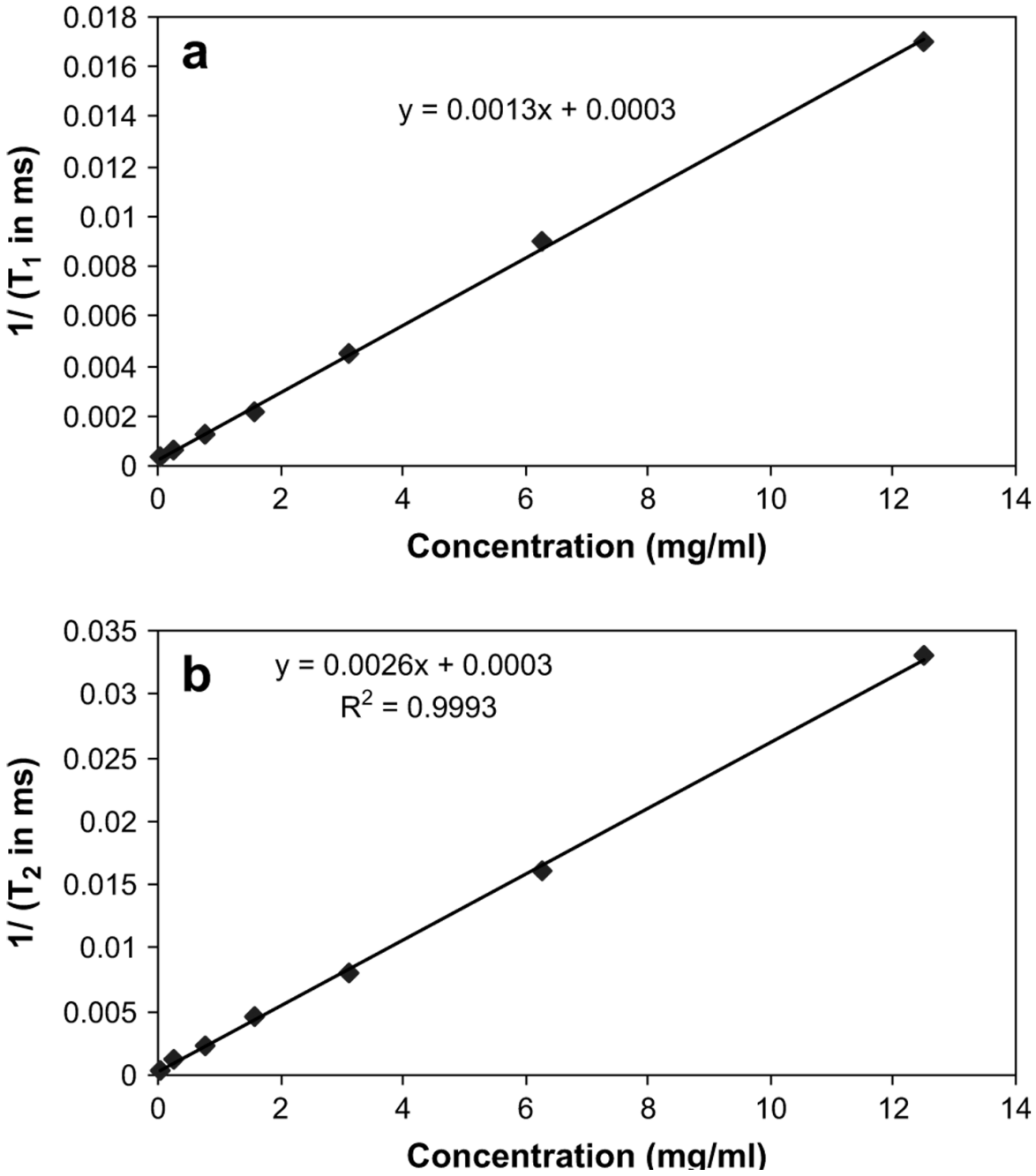

Fig. 1.

(a) Relationship between the inverse of relaxation time (T_1) and Galbumin™ concentration. (b) Relationship between the inverse of relaxation time (T_2) and Galbumin™ concentration. The relaxation times T_1 and T_2 were determined by curve fitting of the signal intensity with respect to the time variables TR and TE using equation (3). For T_1 measurement, MRI images were acquired at 50, 100, 200, 400, 800, 1600, 2400, and 3200 ms TR with TE fixed at 13 ms. For T_2 measurement, TE was 9, 18, 27, 36, 45, 54, 63, 72, and 82 ms with TR fixed at 3000 ms.

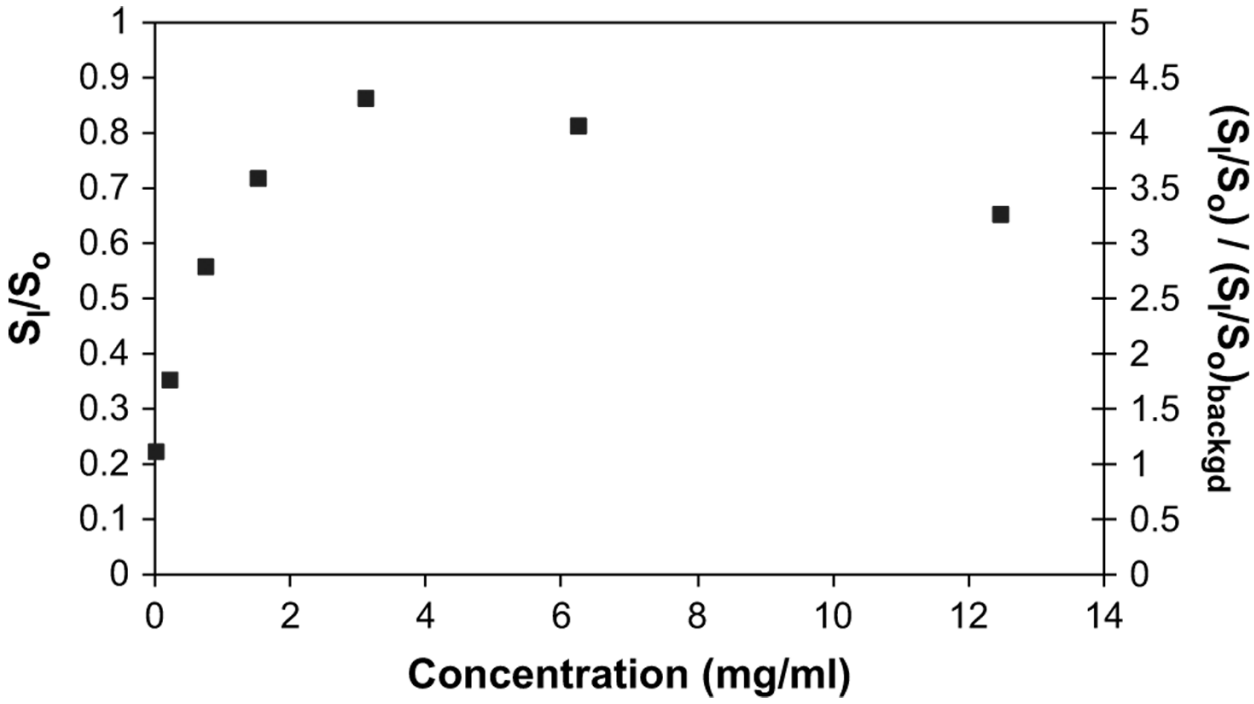

Fig. 2.

Relationship between signal intensity ratio S_I/S_o and Galbumin™ concentration in saline (primary *y*-axis). Relationship between normalized signal intensity ratio of Galbumin™ (S_I/S_o) divided by background (S_I/S_o) and Galbumin™ concentration in saline (secondary *y*-axis). (S_I/S_o) is the signal S_I divided by S_o. The intensity ratios were calculated using the relaxation times T_1 and T_2 at varying Galbumin™ concentration, TR of 675 ms, TE of 13 ms, and equation (3).

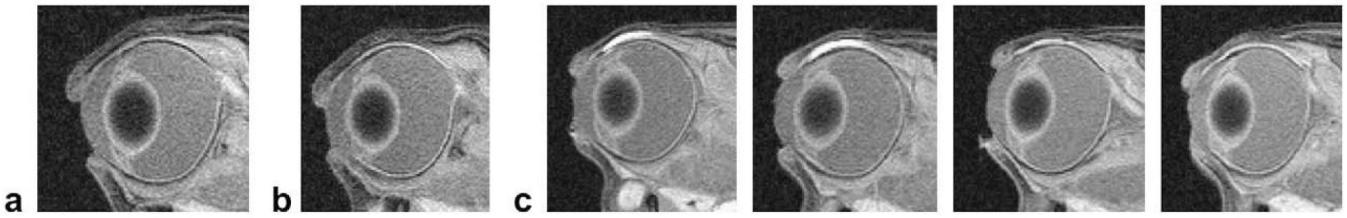

Fig. 3.

Representative MR images of (a) control (no eye treatment), (b) at 50 min after passive delivery (passive control), and (c) at 45 min, 2.5 h, 12.5 h, and 14.5 h, from left to right, respectively, after 20-min 4-mA transscleral iontophoresis of Galbumin™ (concentration in the device ≈ 100 mg/ml) *in vivo*.

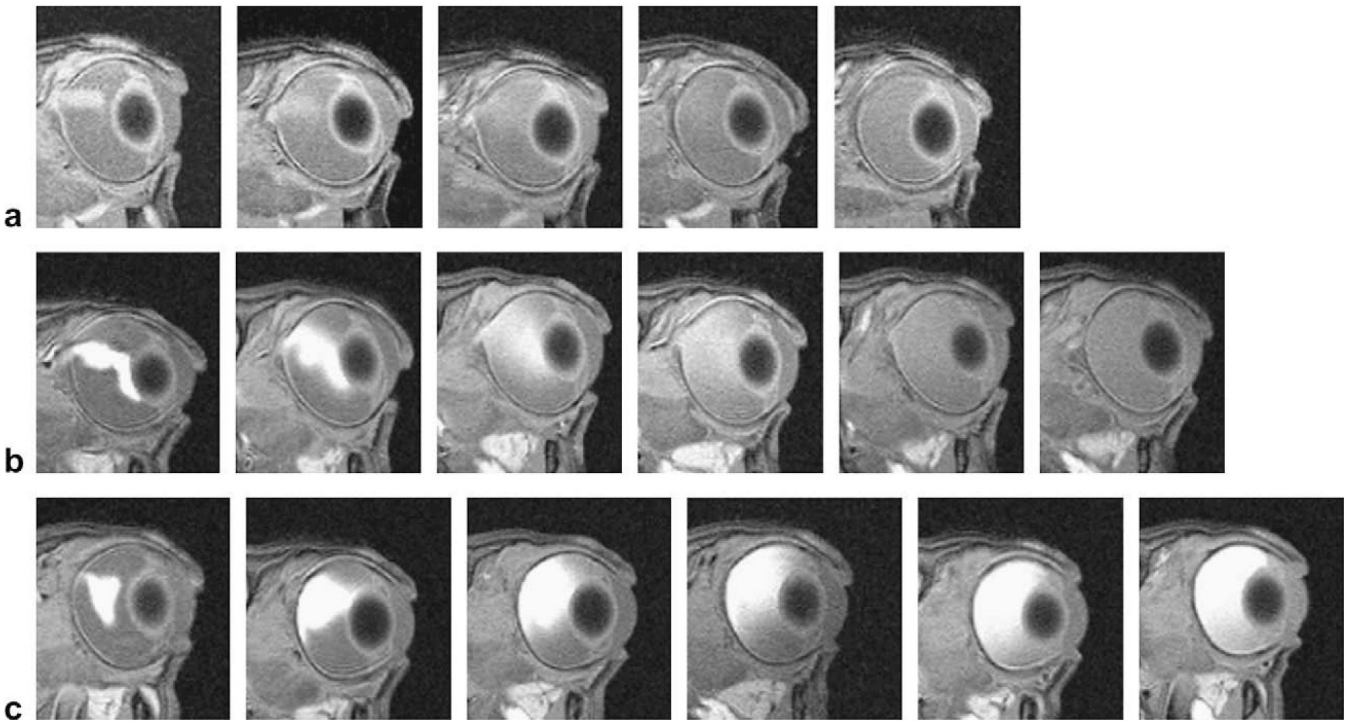

Fig. 4.

Representative MR images after intravitreal injection of (a) 0.25, (b) 1, and (c) 4 mg/ml Galbumin™ *in vivo*. From left to right: (a) at 20 min, 4 h, 7 h, 12 h, and 22 h, (b) at 20 min, 4 h, 13 h, 23.5 h, 39.5 h, and 58.5 h and (c) at 20 min, 4 h, 13 h, 23.5 h, 39.5 h, and 58.5 h, respectively.

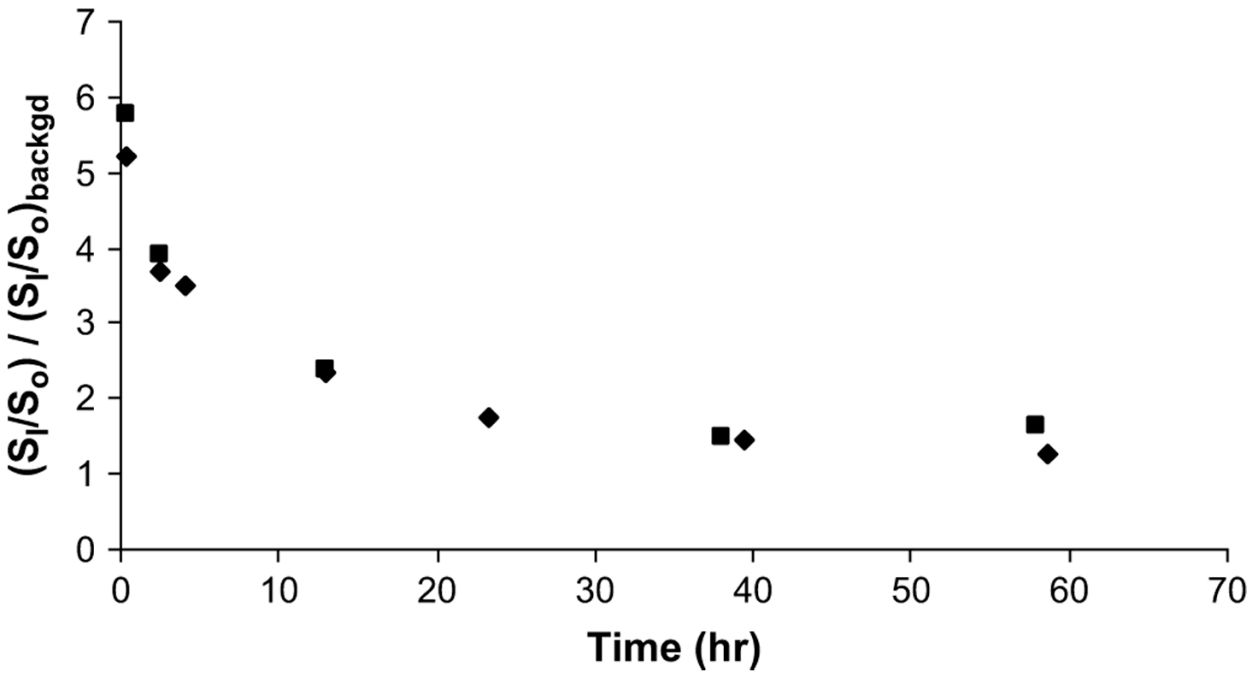

Fig. 5.

$(S_I/S_o)/(S_I/S_o)_{backgd}$ at the region of interest versus time after 1 mg/ml intra-vitreal injection. The ROI is the location of the highest signal in the vitreous – the injection spot. Each symbol represents the data from an individual experiment. $(S_I/S_o)_{backgd}$ is the ratio of the vitreous signal in the absence of contrast agent $(S_I)_{backgd}$, which is approximately 260, to S_o. The ratio of $(S_I/S_o)/(S_I/S_o)_{backgd}$ was determined by S_I and $(S_I)_{backgd}$ and the control signal (usually muscle) in the image slice.

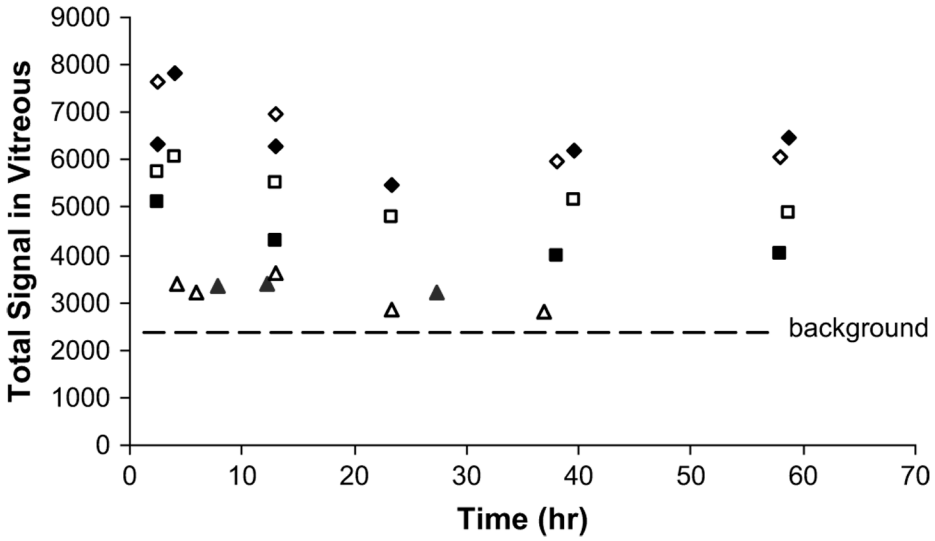

Fig. 6.

Total average signal of the vitreous from the 10 slides covering the majority of the eye after intravitreal injection of 0.25,1, and 4 mg/ml Galbumin™. Total average signal = $\Sigma_{10\ \text{image slides}}$ (average signal of all the voxels in the vitreous in an MR image). Symbols: 0.25 mg/ml, triangles; 1 mg/ml, squares; 4 mg/ml, diamonds. The open and closed symbols represent the data from the replicate under each condition. The line shows the background average signal in the vitreous from 10 slides without the injection.

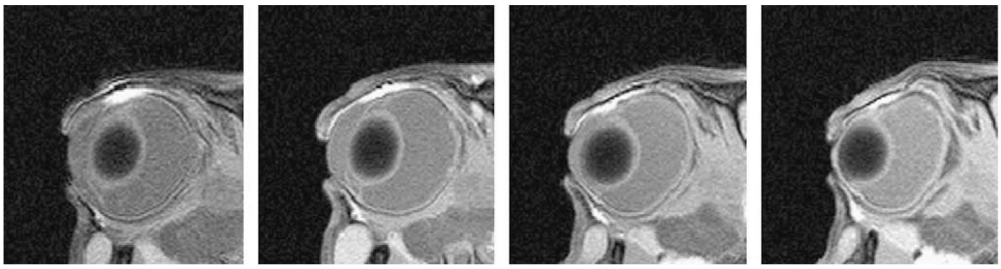

Fig. 7.

Representative MR images at 50 min, 3 h, 13.5 h, and 22.5 h, from left to right, respectively, after 20-min 4-mA transscleral iontophoresis of Galbumin™ (concentration in the device ≈ 100 mg/ml) postmortem.

Table 1

Amounts of Galbumin™ delivered into the eye tissues by 4 mA transscleral iontophoresis for 20 min.

Time after iontophoresis	μg Galbumin™/mg tissue in the conjunctiva (C/M) composite[a]	μg Galbumin™/mg tissue in the sclera (S/C/R) composite[a]	Total μg Galbumin™ in the conjunctiva (C/M) composite	Total μg Galbumin™ in the sclera (S/C/R) composite
30 min	0.13 ± 0.07	0.04 ± 0.02	28 ± 9	13 ± 4
12 h	0.03 ± 0.01	0.02 ± 0.01	3.7 ± 0.8	2.7 ± 2.5

[a] Mean ± SD, $n \geq 3$.